

Disorder-Induced Signal Filtering with Topological Metamaterials

Farzad Zangeneh-Nejad and Romain Fleury*

Disorder, ubiquitously present in realistic structures, is generally thought to disturb the performance of analog wave devices, as it often causes strong multiple scattering effects that largely arrest wave transportation. Contrary to this general view, here, it is shown that, in some wave systems with nontrivial topological character, strong randomness can be highly beneficial, acting as a powerful stimulator to enable desired analog filtering operations. This is achieved in a topological Anderson sonic crystal that, in the regime of dominating randomness, provides a well-defined filtering response characterized by a Lorentzian spectral line-shape. The theoretical and experimental results, serving as the first realization of topological Anderson insulator phase in acoustics, suggest the striking possibility of achieving specific, nonrandom analog filtering operations by adding randomness to clean structures.

The performance of most wave systems, such as lasers, switches, modulators, and signal processors, is largely impeded by disorder. Even at very low concentration, impurities or geometrical imperfections can cause severe self-interference effects, largely hindering wave propagation and device performance. Recently, inspired by the notion of topological insulators (TIs) in condensed matter systems,^[1–3] a fascinating solution to mitigate these harmful consequences has been suggested. TIs are insulating phases with nontrivial topological order, supporting edge states that are resilient to certain types and levels of disorder.^[4–6] Such an unprecedented property, known as topological protection, promises to alleviate the detrimental effects of disorder on wave propagation, enabling the realization of a large variety of topological analog devices that maintain their original functionality even in the presence of impurities.^[7–9]

Although TIs have somewhat enhanced the robustness of analog wave systems to disorder, their topological protection is still limited by a phenomenon, known as Anderson localization (AL).^[10] This process, occurring in the regime with dominating randomness, progressively fills the bandgap of the

TI with disorder-induced localized bulk states, destroying the insulating topological phase and impeding the transportation of the corresponding edge state. Such a behavior seems to be disappointing at first glance because it implies that even topological wave systems become fragile when the disorder level is high enough to turn the TI into an ordinary insulator. Yet, the mere fact that introducing disorder to a system can induce a topological phase transition is encouraging because it suggests that the opposite transition might, in principle, be possible. Recently, in a remarkable development,^[11] it was theoretically demonstrated that some trivial insulators with specific parameters can indeed

go through a topological phase transition upon introducing disorder, converting them to TIs with robust conductive states flowing on their boundaries. Soon after, these exotic topological phases, referred to as disorder-induced topological insulators or topological Anderson insulators (TAIs),^[12–17] were experimentally observed in different physical platforms.^[18–20] Yet, their realization in acoustics has not been reported.

In this work, we provide the first experimental observation of TAI phase in acoustics. We show that the much-sought disorder-induced character of such phases can be leveraged to trigger a well-defined analog filtering operation, namely first-order band-pass filtering.^[21–25] Our findings, defying the conventional view that disorder is detrimental to analog wave systems, hold great promises for a large variety of analog devices in which disorder acts as a powerful engine, forcing the system to perform the functionality of interest.

Let us start with considering the tight-binding toy Hamiltonian of the Su–Schrieffer–Heeger (SSH) chain,^[1] expressed as

$$H = \sum_n \omega_0 a_n^\dagger a_n + \sum_n K a_{2n-1}^\dagger a_{2n} + \sum_n J a_{2n}^\dagger a_{2n+1} + H.C. \quad (1)$$

in which a_n^\dagger and a_n are creation and annihilation operators for the site n , K and J stand, respectively, for the intracell and extracell coupling coefficients and $\omega_0 = 1$ is the on-site energy of the atoms. We suppose that the parameters K and J are defined as $K = K_0 (1 + 0.5 D_s W)$ and $J = J_0 (1 + D_s W)$, in which $K_0 = 0.1$, $J_0 = 0.09$, D_s is a parameter quantifying the strength of disorder, and W is a site-dependent random number. Since $K > J$ in the clean limit ($D_s \rightarrow 0$), the disorder-free system corresponds to a trivial topological phase (BDI symmetry class), characterized by a zero winding number.^[1] To induce a topological phase transition, we start to increase the intrinsic disorder of the system, now considering the case in which $D_s > 0$. Notice that on average,

F. Zangeneh-Nejad, Prof. R. Fleury
 Laboratory of Wave Engineering
 Swiss Federal Institute of Technology in Lausanne (EPFL)
 Lausanne 1015, Switzerland
 E-mail: romain.fleury@epfl.ch

 The ORCID identification number(s) for the author(s) of this article can be found under <https://doi.org/10.1002/adma.202001034>.

© 2020 The Authors. Published by WILEY-VCH Verlag GmbH & Co. KGaA, Weinheim. This is an open access article under the terms of the Creative Commons Attribution License, which permits use, distribution and reproduction in any medium, provided the original work is properly cited.

DOI: 10.1002/adma.202001034

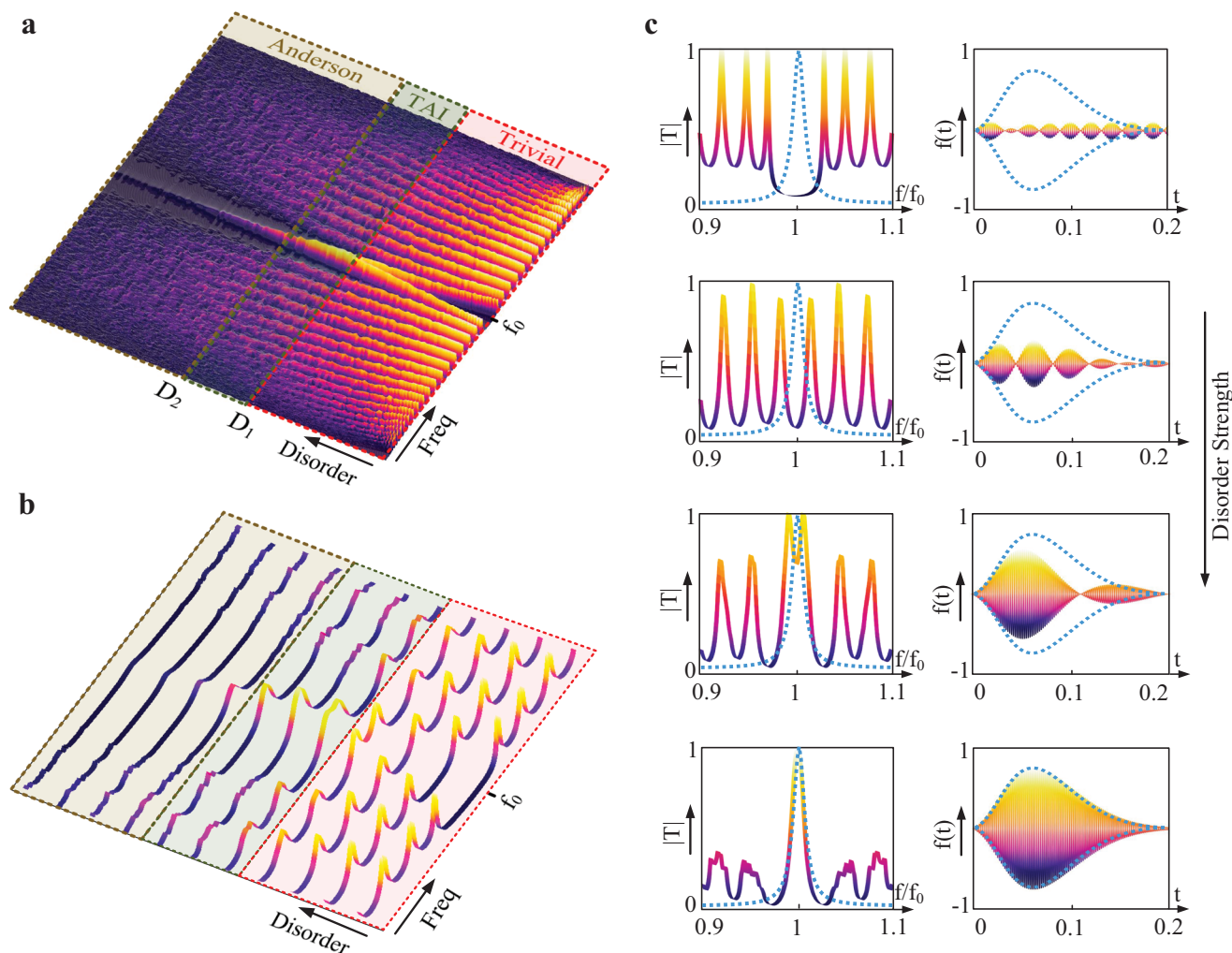


Figure 1. Disorder-induced analog signal filtering based on topological Anderson insulators. We consider the disordered version of Su–Schrieffer–Heeger (SSH) model, described by the tight-binding toy model given in Equation (1) with the specified parameters, and build a two-port scattering system by coupling a finite crystal piece with 100 unit cells to two external waveguides. a) Evolution of the corresponding (averaged) transmission spectrum versus disorder strength. Starting from an ordinary trivial insulator in the clean limit (red region), the system switches into a topological insulator in the regime $D_1 < D_s < D_2$ (TAI regime), characterized by a zero-energy edge state which manifests itself as a resonance peak in the spectrum. For extremely high disorder intensities (yellow region), the transportation is arrested by Anderson localization. b) Averaged transmission coefficient of the system for several representative disorder strengths. In the TAI regime (green area), the spectrum exhibits a Lorentzian profile near f_0 , corresponding to the transfer function of a first-order band-pass filter. c) Demonstration of disorder-induced analog filtering. We suppose that the system is excited with a Gaussian-modulated sinusoidal signal and calculate the corresponding transmission coefficient (T) and output time signal ($f(t)$), when gradually increasing the disorder strength from zero to the regime of TAI. It is seen that disorder acts like an actuator in our system, applying the desired filtering operation to the input signal.

regardless of D_s , the parameter K is always smaller than J . Yet, and quite surprisingly, the difference in their standard deviations can create a topological phase transition in a certain range of values for D_s (see Note SI, Supporting Information), leading to an insulator with nontrivial topological index (nonzero winding number). In order to examine such a possibility, we consider a finite two-port scattering system made of 100 unit cells coupled to external waveguides and report in **Figure 1a** the disorder-averaged transmission spectrum versus the parameter D_s (see Note SII, Supporting Information, for the numerical methods). As observed, in the disorder-free case, the spectrum is gapped around f_0 . This insulating bandgap becomes narrower with increasing disorder strength and is eventually closed at $D_1 = 1.68$. After D_1 (and before $D_2 = 3.64$), the bandgap reopens but, this

time, it includes a resonance peak emerging at the center of the gap. This in-gap resonance, corresponding to resonant tunneling through a topological edge state, indicates the nontrivial character of the system under investigation for $D_1 < D_s < D_2$ (TAI regime). If one increases the disorder level further ($D_s > D_2$), the onset of AL is reached, where all states start to localize in the bulk with decreasing transmission coefficient. In **Figure 1b**, we have plotted the disorder-averaged transmission coefficient for several representative disorder strengths. Notice that, in the TAI regime, the topological mid-gap resonance has a Lorentzian profile, following the general form of $H(\omega) = A/(Bj(\omega - \omega_0) + C)$ in the vicinity of ω_0 . Remarkably, $H(\omega)$ corresponds to the transfer function of a first-order band-pass filter. It then follows that our disordered 1D toy model acts as a first-order analog filter, induced by disorder.

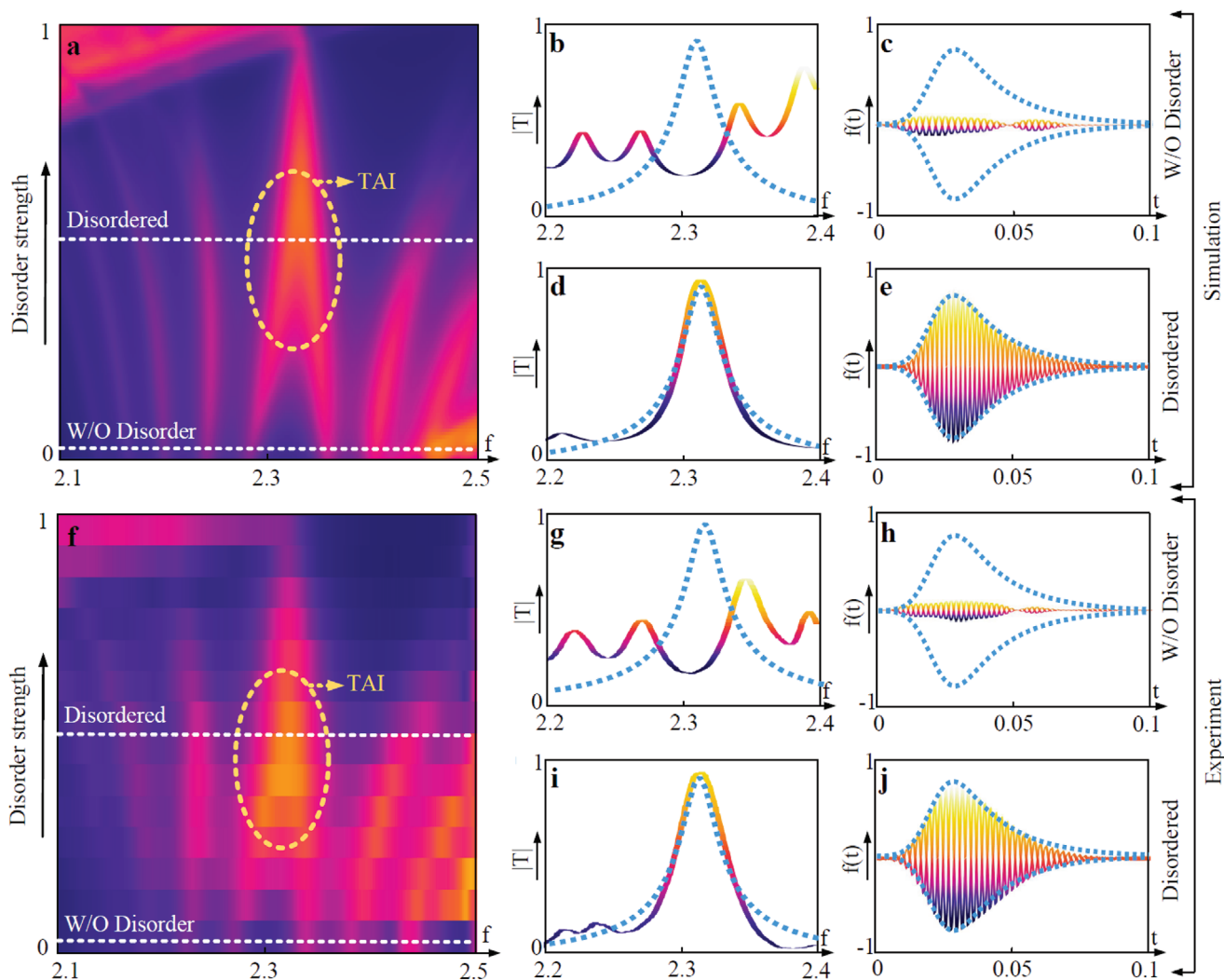


Figure 2. Experimental demonstration of acoustic topological Anderson insulators and disorder-induced analog filtering. We map the proposed tight-binding toy model into a 1D sonic crystal, based on coupled acoustic quasi-bound states in the continuum. a) Evolution of the (averaged) transmission coefficient of the phononic crystal as the strength of disorder is increased, obtained via 3D full-wave numerical simulations. The emergence of a disorder-induced zero-energy state is clear in the disorder-averaged transmission spectrum (oval region), allowing one to perform a well-defined first-order filtering operation. b,c) Disorder-averaged transmission spectrum and the corresponding transmitted field (numerical simulations), when the disordered-free system is excited with a Gaussian time-modulated signal. d,e) Same as (b) and (c) except that the system is sufficiently disordered, so that it finds itself in the TAI regime. f–j) Experimental measurements corresponding to the simulation results.

In particular, while the system under study is performing a definite task, it has a disorder-induced character and an indefinite randomly drawn geometry, a property that directly stems from the underlying topological Anderson insulator phase.

In order to examine the functionality of the proposed system, we assume that the system is excited with a Gaussian-modulated sinusoidal pulse (see Note SIII, Supporting Information, for other forms of excitation signals) and calculate the corresponding disorder-averaged transmitted signal ($f(t)$) and transmission spectrum (T), when gradually increasing the disorder level from zero to the regime of TAI. The corresponding results are depicted in Figure 1c, illustrating how random disorder forces the proposed system to apply a definite first-order filtering operation to the input signal, leading to the desired output signal (marked with blue color).

To validate these findings in a full-wave 3D geometry, we map the proposed tight-binding model into a 1D phononic crystal, built from a chain of acoustic quasi-bound states in the continuum (BICs)^[26–29] embedded in a monomode acoustic waveguide. Such coupled bound states, resonating at the frequency of $f_0 = 2310$ Hz, mimic the evanescently coupled tight-binding chain described by the Hamiltonian of Equation (1). This leads to the realization of an acoustic topological Anderson insulator that, in the regime of dominating randomness, supports zero-energy edge modes. Note that, to the best of our knowledge, the realization of topological Anderson insulator phase in acoustics has not been reported elsewhere. In order to probe the proposed system with far-field scattering tests based on the waveguide mode, we make the radiative quality factor of the bound states finite by slightly

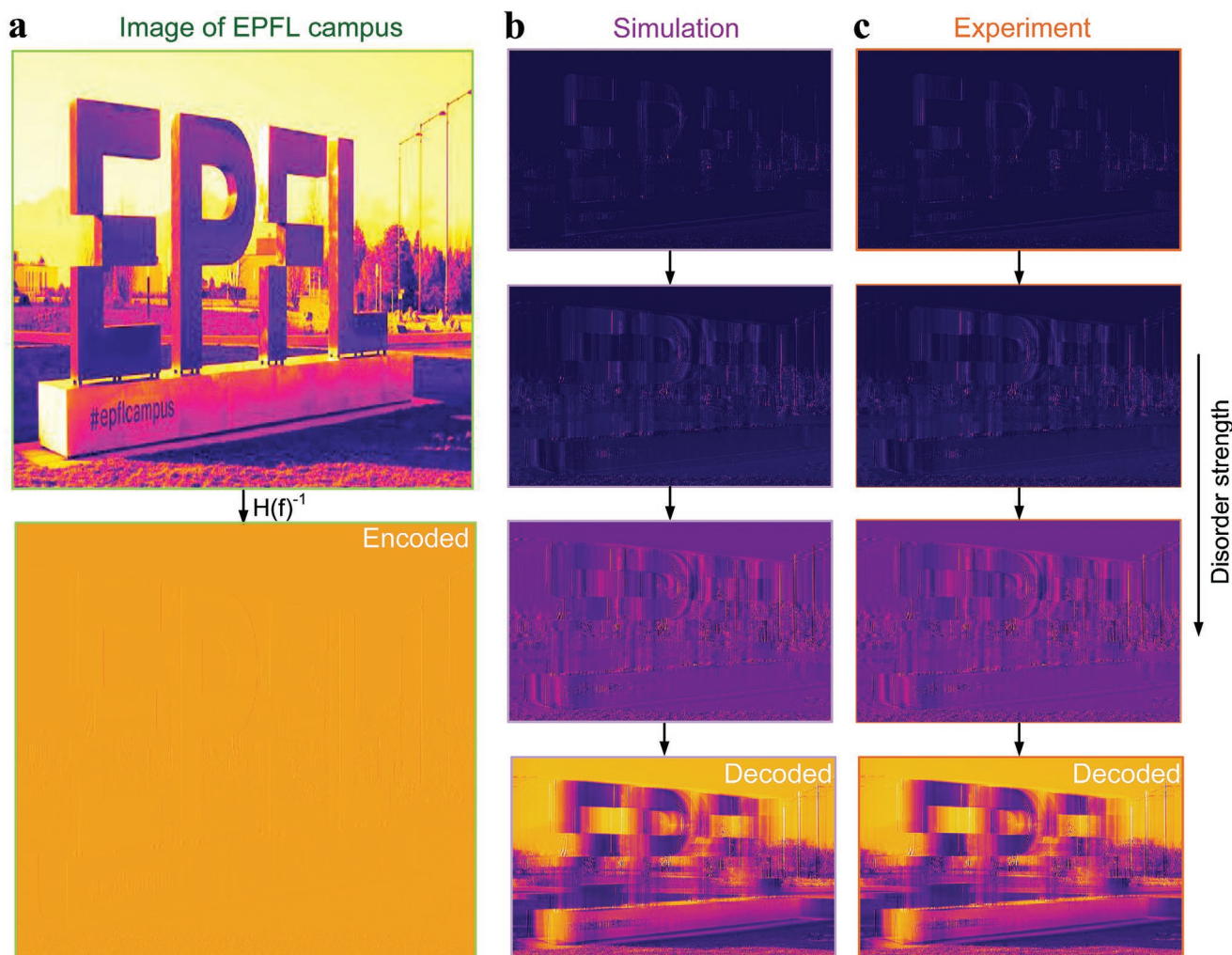


Figure 3. Disorder-induced analog filtering of an image. a) (Top) Image of the EPFL campus and (bottom) the original image is encrypted with the inverse of the target filtering function $H(f)$. The encrypted image is then fed into the input of the proposed topological Anderson system. b) Corresponding output images as the level of disorder is gradually increased. Since in the regime of TAI, the transfer function of the system is approximately equal to $H(f)$, the corresponding output is nothing but the decrypted image. c) Corresponding experimental results. The results, in agreement with numerical simulations, demonstrate the intriguing possibility of decoding the encrypted image by providing the system with more and more disorder.

breaking the inversion symmetry of the structure with respect to its longitudinal axis.

Figure 2a represents the transmission coefficient (averaged over disorder realizations) as a function of both frequency and disorder strength, obtained via 3D full-wave numerical simulations based on the finite element method. The result of this figure confirms the emergence of a disorder-induced resonance peak, corresponding to the zero-energy state of the TAI phase (the oval region). The possibility to leverage the Lorentzian line shape of this resonance for carrying out disorder-induced filtering is demonstrated in Figures 2b–e, where we have reported the averaged transmittance of the system both in the clean limit and in the topological Anderson phase. When no disorder is imparted to the system, the transmission spectrum (Figure 2b) exhibits a minimum due to a bandgap around f_0 , leading to an output

signal (Figure 2c) that has an almost zero amplitude (the blue curve, which is analytically predicted). In the regime of TAI phase, on the contrary, the transmission spectrum matches the desired transfer function $H(f)$ (Figure 2d), corresponding to a first-order analog filter. As such, the corresponding transmitted signal, shown in Figure 2e, follows well the targeted filtered signal (the blue curve). The experimental measurements corresponding to these numerical findings, provided respectively in Figures 2f–j, are in perfect agreement with the simulations. Importantly, the reported results are averaged over multiple realizations of disorder and the standard deviation, which is inversely proportional to the system size, is kept at a small level. Note that, in principle, it is possible to achieve more complex higher-order filtering operations by constructing a network of several realizations of the proposed first-order filter (see Note SIV, Supporting Information).

The proposed disorder-induced acoustic filter can be used to manipulate the spectral characteristics of 2D signals, i.e., images, as well. Consider the image of the EPFL campus, shown in Figure 3a (top). Suppose that the pixels of this image are processed by the inverse of the target filtering function $H(f)$, therefore encrypting the image. We excite the proposed system with a signal corresponding to the encrypted image. Since, in the regime of TAI, the transfer function of the proposed system is approximately equal to $H(f)$, the system is expected to decrypt the encoded image. This is demonstrated in the insets of Figure 3b, illustrating how the encrypted image signal is gradually decoded by the proposed topological Anderson system, when more and more disorder is introduced. The associated experimental results, shown in Figure 3c, are in full agreement with the simulations. Note that decoding the image is not a trivial task as one needs not only to tune the disorder strength to the right level, but also to have some information about the required disorder statistics, in particular the difference in the standard deviations of the couplings. We note that the proposed system can be used for image edge detection as well (see Note SIV, Supporting Information).

In summary, we demonstrated a novel scheme for analog signal filtering, in which random disorder drives the system, forcing it to realize the desired filtering operation. Although demonstrated here in the context of acoustics, we expect the emergence of such spectral filters to be generic. In Note SV in the Supporting Information, we demonstrate a photonic instance. Not only do our findings serve as the first experimental observation of topological Anderson insulator phase in acoustics but also they open a new horizon for realizing a new generation of analog wave filters that rely on disorder. This is in sharp contrast to ordinary trivial analog filters in which disorder is highly detrimental (see Note SVII, Supporting Information).

Experimental Section

Figure S1 in the Supporting Information shows a photograph of the fabricated prototype of the proposed topological sonic crystal. The sample includes a transparent pipe with square transverse cross-section, serving as a waveguide, and a chain of scatterers, that are embedded inside the waveguide. The scatterers used in the sample are commercially available Nylon 6 cast plastic rods. The width, height, and length of the waveguide are $W = 7$ cm, $H = 7$ cm, $L = 2$ m, respectively, the radii of the cylinders are $R = 1.75$ cm, the lattice constant is $a = 16.6$ cm, and the detuning parameter is $d = 7.8$ cm. The structure is tested in the experimental setup shown in Figure S2 in the Supporting Information. Apart from the fabricated prototype, the setup includes three PCB 130F20 ICP microphones, measuring the associated pressure field, a loudspeaker, generating sound and exciting the system, an acoustic Quattro Data physic analyzer, recording the associated measured data, and a computer, controlling the setup. Note also that, in order to avoid unwanted reflection and refraction, the end of the system is terminated with an anechoic termination, made of adiabatically tapered foam, shown in the bottom panel of the figure. In order to extract the disorder-averaged transmission coefficient, the system was excited with the loudspeaker and the corresponding transmission spectrum was extracted for each realization of disorder by standard standing wave pattern analysis. Then, the average of ten different independent measurements was taken, each of which corresponds to a distinct disorder configuration.

Supporting Information

Supporting Information is available from the Wiley Online Library or from the author.

Acknowledgements

This work was supported by the Swiss National Science Foundation (SNSF) under Grant No. 172487.

Conflict of Interest

The authors declare no conflict of interest.

Keywords

acoustics, Anderson localization, metamaterials, topological insulators

Received: February 13, 2020

Revised: April 9, 2020

Published online:

- [1] M. Z. Hasan, C. L. Kane, *Rev. Mod. Phys.* **2010**, *82*, 3045.
- [2] C. He, X. Ni, H. Ge, X. Sun, Y. Chen, M. Lu, X. Liu, Y. Chen, *Nat. Phys.* **2016**, *12*, 1124.
- [3] G. Ma, M. Xiao, C. T. Chan, *Nat. Rev. Phys.* **2019**, *1*, 281.
- [4] X. Cheng, C. Jouvaud, X. Ni, S. H. Mousavi, A. Z. Genack, A. B. Khanikaev, *Nat. Mater.* **2016**, *15*, 542.
- [5] S. Yves, R. Fleury, T. Berthelot, M. Fink, F. Lemoult, G. Lerosey, *Nat. Commun.* **2017**, *8*, 16023.
- [6] A. Slobozhanyuk, S. H. Mousavi, X. Ni, D. Smirnova, Y. S. Kivshar, A. B. Khanikaev, *Nat. Photonics* **2017**, *11*, 130.
- [7] F. Zangeneh-Nejad, R. Fleury, *Nat. Commun.* **2019**, *10*, 2058.
- [8] M. A. Bandres, S. Wittek, G. Harari, M. Parto, J. Ren, M. Segev, D. N. Christodoulides, M. Khajavikhan, *Science* **2018**, *359*, eaar4005.
- [9] F. Zangeneh-Nejad, R. Fleury, *Phys. Rev. Lett.* **2019**, *123*, 053902.
- [10] M. Segev, Y. Silberberg, D. N. Christodoulides, *Nat. Photonics* **2013**, *7*, 197.
- [11] J. Li, R. Chu, J. K. Jain, S. Shen, *Phys. Rev. Lett.* **2009**, *102*, 136806.
- [12] A. Altland, D. Bagrets, L. Fritz, A. Kamenev, H. Schmiedt, *Phys. Rev. Lett.* **2014**, *112*, 206602.
- [13] C. B. Hua, R. Chen, D. H. Xu, B. Zhou, *Phys. Rev. B* **2019**, *100*, 205302.
- [14] F. Cardano, A. D'Errico, A. Dauphin, M. Maffei, B. Piccirillo, C. de Lisio, G. De Filippis, V. Cataudella, E. Santamato, L. Marrucci, M. Lewenstein, P. Massignan, *Nat. Commun.* **2017**, *8*, 15516.
- [15] I. Mondragon-Shem, T. L. Hughes, J. Song, E. Prodan, *Phys. Rev. Lett.* **2014**, *113*, 046802.
- [16] X. Ni, K. Chen, M. Weiner, D. J. Apigo, C. Prodan, A. Alù, E. Prodan, A. B. Khanikaev, *Commun. Phys.* **2019**, *2*, 1.
- [17] K. Chen, M. Weiner, M. Li, X. Ni, A. Alù, A. B. Khanikaev. **2019**, arXiv preprint arXiv:1912.06339.
- [18] S. Stützer, Y. Plotnik, Y. Lumer, P. Titum, N. H. Lindner, M. Segev, M. C. Rechtsman, A. Szameit, *Nature* **2018**, *560*, 461.
- [19] E. J. Meier, F. A. An, A. Dauphin, M. Maffei, P. Massignan, T. L. Hughes, B. Gadway, *Science* **2018**, *362*, 929.
- [20] Z. Q. Zhang, B. L. Wu, J. Song, H. Jiang, *Phys. Rev. B* **2019**, *100*, 184202.
- [21] A. Pors, M. G. Nielsen, S. I. Bozhevolnyi, *Nano Lett.* **2015**, *15*, 791.

- [22] H. Kwon, D. Sounas, A. Cordaro, A. Polman, A. Alù, *Phys. Rev. Lett.* **2019**, *121*, 173004.
- [23] F. Zangeneh-Nejad, R. Fleury, *New J. Phys.* **2018**, *20*, 073001.
- [24] A. Cordaro, H. Kwon, D. Sounas, A. F. Koenderink, A. Alù, A. Polman, *Nano Lett.* **2019**, *19*, 8418.
- [25] T. Yang, J. Dong, L. Lu, L. Zhou, A. Zheng, J. Chen, *Sci. Rep.* **2015**, *4*, 5581.
- [26] A. Kodigala, T. Lepetit, Q. Gu, B. Bahari, Y. Fainman, B. Kanté, *Nature* **2017**, *541*, 196.
- [27] F. Zangeneh-Nejad, R. Fleury, *Rev. Phys.* **2019**, *4*, 100031.
- [28] M. Molina, A. E. Miroshnichenko, Y. S. Kivshar, *Phys. Rev. Lett.* **2012**, *108*, 070401.
- [29] F. Zangeneh-Nejad, R. Fleury, *Phys. Rev. Lett.* **2019**, *122*, 014301.